

Highly Pathogenic Avian Influenza A(H5N8) Virus in Swans, China, 2020

Xiang Li,¹ Xinru Lv,¹ Yi Li,¹ Peng Peng, Ruifang Zhou, Siyuan Qin, Enda Ma, Wenqiang Liu, Tian Fu, Peiran Ma, Qing An, Yiran Li, Yuping Hua, Yulong Wang, Chengliang Lei, Dong Chu, Heting Sun, Yanbing Li, Yuwei Gao, Hongliang Chai

Author affiliations: Northeast Forestry University College of Wildlife and Protected Area, Harbin, China (X. Li, X. Lv, Y. Li, T. Fu, P. Ma, Q. An, Yiran Li, Y. Hua, Y. Wang, H. Chai); General Station for Surveillance of Wildlife Disease and Wildlife Borne Diseases, National Forestry and Grassland Administration, Shenyang, China (P. Peng, S. Qin, D. Chu, H. Sun); Bayannur Desert Comprehensive Management Center, Bayannur Forestry Scientific Research Institute, Bayannur, China (R. Zhou); Wildlife and Wetland Conservation Center, Bayannur Forestry and Grassland Administration, Bayannur (E. Ma, W. Liu); State Key Laboratory of Veterinary Biotechnology, Harbin Veterinary Research Institute, Harbin (Yanbing Li); National Forestry and Grassland Administration Department of Wildlife Protection, Beijing, China (C. Lei); Military Veterinary Research Institute of Academy of Military Medical Sciences, Changchun, China (Y. Gao)

DOI: <https://doi.org/10.3201/eid2706.204727>

In October 2020, highly pathogenic avian influenza A(H5N8) viruses were detected in 2 dead swans in Inner Mongolia, China. Genetic analysis showed that the H5N8 isolates belong to clade 2.3.4.4b and that the isolates cluster with the H5N8 viruses isolated in Eurasia in the fall of 2020.

Since 2008, highly pathogenic avian influenza (HPAI) H5 clade 2.3.4 viruses with various neuraminidase combinations have been identified, and these subtypes have subsequently evolved into different subclades, including clade 2.3.4.4 (1–3). In contrast to the 2014–2015 H5N8 clade 2.3.4.4 viruses, which spread worldwide through wild migratory birds (4), the intercontinental spread of clade 2.3.4.4b viruses began in fall 2016 (5). Moreover, clade 2.3.4.4b viruses have had a sustained prevalence in Europe, Africa, and the Middle East in recent years (<https://www.oie.int/en/animal-health-in-the-world>). In January 2020, clade 2.3.4.4h of HPAI A(H5N6) virus was detected in whooper swans (*Cygnus cygnus*) and mute swans (*C. olor*) in Xinjiang (6); however, no outbreaks of H5N8 in mainland China have been reported since 2017. We

report the reemergence of HPAI H5N8 viruses from wild aquatic birds in mainland China.

On October 17, 2020, we collected multiple organs (brains, larynx, liver, lung, pancreas, kidney, spleen, and rectum) from 2 dead swans, a whooper swan and a mute swan, in Wuliangshuai Lake in Bayannur City, Inner Mongolia, China (40.95138889°N, 108.9266667°E) (Figure). We sequenced the H5N8 genomes directly from organs. We isolated 2 H5N8 influenza viruses, A/whooper swan/Inner Mongolia/W1-1/2020(H5N8) and A/mute swan/Inner Mongolia/W2-1/2020(H5N8).

We sequenced the full-length genomes and confirmed that the 2 isolates were HPAI viruses on the basis of the amino acid sequence REKRRKR↓GLFGAI at the hemagglutinin cleavage site. The sequences of these 2 Inner Mongolia H5N8 isolates (IM-H5N8) were deposited into the GISAID database (<http://www.gisaid.org>; accession nos. EP11811641–56). The receptor-binding site at the 222–224 (H5 numbering) motif (QRG) suggested avian-like (α 2–3-SA) receptors, and the substitutions D94N, S123P, and S133A (H5 numbering), which are associated with increased binding to human-like (α 2–6-SA) receptors, were identified. The residues Q591, E627, and D701 in the polymerase basic 2 protein suggest that these viruses have not yet adapted to mammalian hosts.

Sequence comparisons showed high nucleotide identity across all 8 gene segments between the 2 IM-H5N8 isolates (99.8%–100%). A BLAST search (<https://blast.ncbi.nlm.nih.gov/Blast.cgi>) performed in the GISAID database suggested that IM-H5N8 shares the highest nucleotide identity (>99%) with the H5N8 viruses isolated in Eurasia in fall 2020 (EA-H5N8) (Appendix Table 1, <https://wwwnc.cdc.gov/EID/article/27/6/20-4727-App1.pdf>). These results indicate that IM-H5N8 and EA-H5N8 are descendants of a common ancestral virus. Phylogenetic analysis further confirmed that the 8 segments had a common evolutionary source, clustering with EA-H5N8 and belonging to clade 2.3.4.4b (Appendix Figure).

Clade 2.3.4.4b H5N8 viruses were detected mainly in poultry in Europe in early 2020 but were not related to IM-H5N8 (Appendix Figure) (7). On May 12 2020, IM-H5N8 like virus was first detected in poultry in Iraq (7). It might be the source of IM-H5N8-like viruses. Soon after, similar viruses were reported in southern central Russia in late July 2020, and they jumped into wild birds in September in Russia and Kazakhstan (Appendix Table 1). Migratory birds moving within several flyways in Eurasia have overlapping breeding areas (8), and breeding origin

¹These first authors contributed equally to this article.

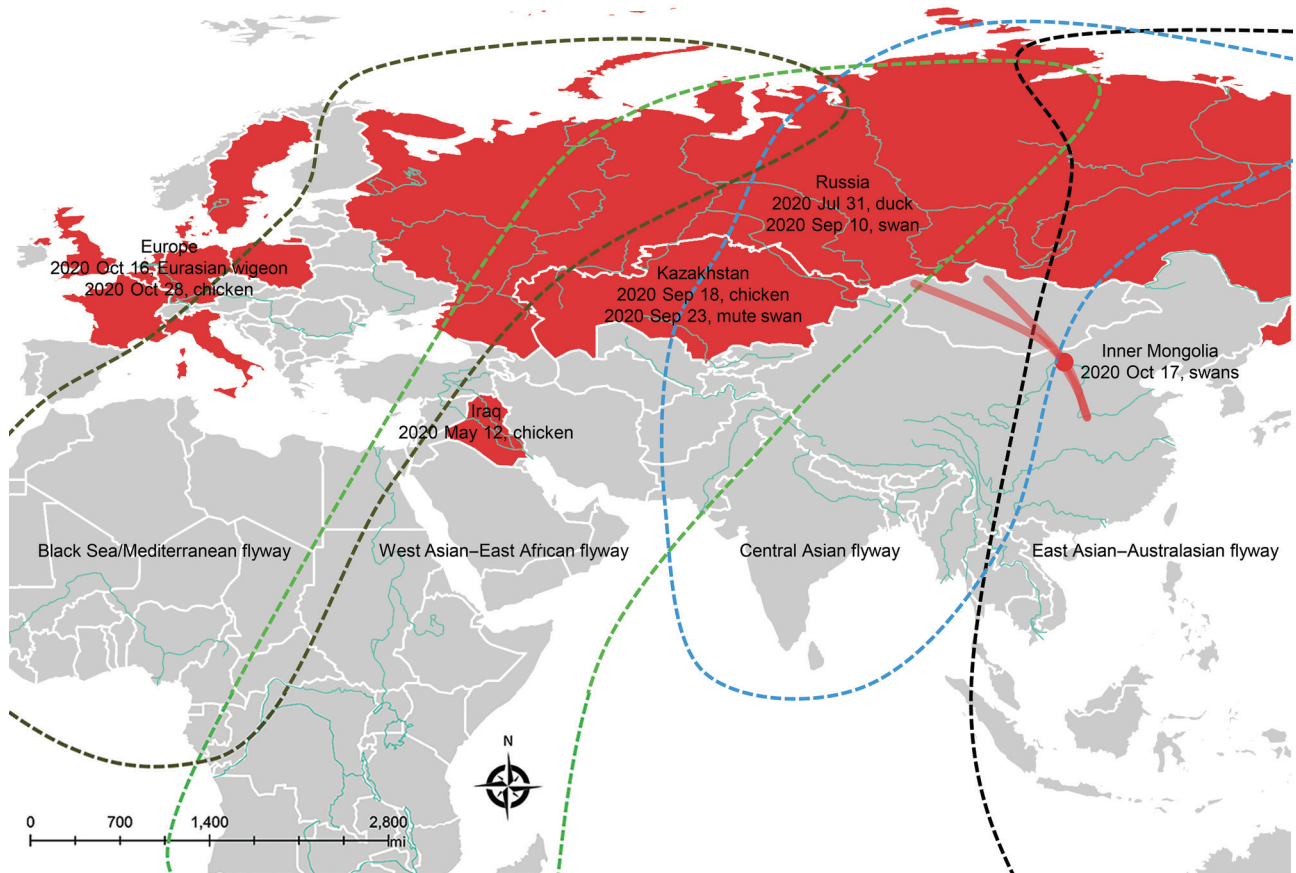


Figure. Global distribution of the influenza A(H5N8) viruses related to 2 H5N8 isolates detected in whooper swans (*Cygnus cygnus*) and mute swans (*C. olor*) in Inner Mongolia, China, 2020. Red dot indicates sampling site in Inner Mongolia; red solid lines indicate whooper swan migratory routes in central China. Dates refer to the day of initial H5N8 virus isolated in poultry and wild birds in each country in 2020.

assignments suggest that migration distances vary by a maximum of $\approx 3,500$ km (9). Such a unique ecosystem could be implicated as a pathway for the cross-regional spread of HPAI viruses during the autumn migration of waterfowl. Birds breeding in Russia that migrate along different routes might be responsible for the widespread transmission of H5N8 viruses in both Europe and China in fall 2020.

The migration routes of whooper swans along the Central Asian flyway have been identified (10); the widely distributed lakes in western and northern Mongolia (including the lakes in Russia near Mongolia) are important breeding areas, and Inner Mongolia (including Bayannur City, Baotou City, and Ordos City) and Shaanxi (including Yulin City) are the key stopover sites during the migration of whooper swans in China. Whooper swans usually winter along the Yellow River (e.g., in Henan [Sanmenxia Reservoir area] and Shanxi [Shengtian Lake]), and whooper swans also wander between different wintering grounds. Despite no reported outbreak of

HPAI A(H5N8) virus in Mongolia, Russia reported a similar swan outbreak of HPAI A(H5N8) virus on August 28, 2020 (https://www.oie.int/wahis_2/temp/reports/en_fup_0000035737_20200915_110259.pdf), which could be the source of the infections in these swans in Bayannur City in Inner Mongolia through swan migration.

In conclusion, we detected HPAI A(H5N8) during the autumn migration of whooper swans through Inner Mongolia. This finding warrants strengthening the monitoring of HPAI A(H5N8) in swans and other migratory waterfowl in the main stopover sites and wintering grounds, especially in the Sanmenxia Reservoir area in Henan Province.

Acknowledgments

We thank the authors and submitting laboratories of the sequences from the GISAID EpiFlu Database.

This study was funded by the National Natural Science Foundation of China (grant no. 31970501) and by the

Surveillance of Wildlife Diseases from the National Forestry and Grassland Administration.

About the Author

Mr. Li is a graduate student at the College of Wildlife and Protected Area at Northeast Forestry University in Heilongjiang, China. His primary research interest is the epidemiology of influenza viruses.

References

1. Gu M, Liu W, Cao Y, Peng D, Wang X, Wan H, et al. Novel reassortant highly pathogenic avian influenza (H5N5) viruses in domestic ducks, China. *Emerg Infect Dis*. 2011;17:1060–3. <https://doi.org/10.3201/eid1706.101406>
2. Wu H, Peng X, Xu L, Jin C, Cheng L, Lu X, et al. Novel reassortant influenza A(H5N8) viruses in domestic ducks, eastern China. *Emerg Infect Dis*. 2014;20:1315–8. <https://doi.org/10.3201/eid2008.140339>
3. Cui Y, Li Y, Li M, Zhao L, Wang D, Tian J, et al. Evolution and extensive reassortment of H5 influenza viruses isolated from wild birds in China over the past decade. *Emerg Microbes Infect*. 2020;9:1793–803. <https://doi.org/10.1080/22221751.2020.1797542>
4. Global Consortium for H5N8 and Related Influenza Viruses. Role for migratory wild birds in the global spread of avian influenza H5N8. *Science*. 2016;354:213–7. <https://doi.org/10.1126/science.aaf8852>
5. Li M, Liu H, Bi Y, Sun J, Wong G, Liu D, et al. Highly pathogenic avian influenza A(H5N8) virus in wild migratory birds, Qinghai Lake, China. *Emerg Infect Dis*. 2017;23:637–41. <https://doi.org/10.3201/eid2304.161866>
6. Li Y, Li M, Li Y, Tian J, Bai X, Yang C, et al. Outbreaks of highly pathogenic avian influenza (H5N6) virus subclade 2.3.4.4h in swans, Xinjiang, western China, 2020. *Emerg Infect Dis*. 2020;26:2956–60. <https://doi.org/10.3201/eid2612.201201>
7. Lewis NS, Banyard AC, Whittard E, Karibayev T, Al Kafagi T, Chvala I, et al. Emergence and spread of novel H5N8, H5N5 and H5N1 clade 2.3.4.4 highly pathogenic avian influenza in 2020. *Emerg Microbes Infect*. 2021;10:148–51. <https://doi.org/10.1080/22221751.2021.1872355>
8. Saito T, Tanikawa T, Uchida Y, Takemae N, Kanehira K, Tsunekuni R. Intracontinental and intercontinental dissemination of Asian H5 highly pathogenic avian influenza virus (clade 2.3.4.4) in the winter of 2014–2015. *Rev Med Virol*. 2015;25:388–405. <https://doi.org/10.1002/rmv.1857>
9. Sorensen MC, Dixit T, Kardynal KJ, Newton J, Hobson KA, Bensch S, et al. Migration distance does not predict blood parasitism in a migratory songbird. *Ecol Evol*. 2019;9:8294–304. <https://doi.org/10.1002/ece3.5404>
10. Li S, Meng W, Liu D, Yang Q, Chen L, Dai Q, et al. Migratory whooper swans *Cygnus cygnus* transmit H5N1 virus between China and Mongolia: combination evidence from satellite tracking and phylogenetics analysis. *Sci Rep*. 2018;8:7049. <https://doi.org/10.1038/s41598-018-25291-1>

Address for correspondence: Hongliang Chai, College of Wildlife and Protected Area, Northeast Forestry University, No. 26 Hexing Rd, Xiangfang District, Harbin 150040, Heilongjiang, China; email: hongliang_chai@hotmail.com

Rapid Antigen Test for Postmortem Evaluation of SARS-CoV-2 Carriage

Martin Zacharias, Verena Stangl, Andrea Thüringer, Martina Loibner, Philipp Wurm, Stella Wolfgruber, Kurt Zatloukal, Karl Kashofer, Gregor Gorkiewicz

Author affiliation: Medical University of Graz, Graz, Austria

DOI: <https://doi.org/10.3201/eid2706.210226>

Detecting severe acute respiratory syndrome coronavirus 2 in deceased patients is key when considering appropriate safety measures to prevent infection during postmortem examinations. A prospective cohort study comparing a rapid antigen test with quantitative reverse transcription PCR showed the rapid test's usability as a tool to guide autopsy practice.

Rapid detection of severe acute respiratory syndrome coronavirus 2 (SARS-CoV-2) is essential to prevent viral dissemination. Rapid antigen tests (RATs) have recently been approved and are now widely used in the current coronavirus disease (COVID-19) pandemic (1). Although the performance of RATs has been evaluated extensively in clinics (2–4), data on postmortem testing are still lacking (5).

We performed a prospective cohort study in which we evaluated the performance of the Roche/SD Biosensor SARS-CoV-2 RAT (<https://www.roche.com>) in 30 consecutive deceased COVID-19 patients at the University Hospital, Medical University of Graz (Graz, Austria), during November 28–December 23, 2020. We tested each corpse with nasopharyngeal swabs for RAT (using the manufacturer's kit) and eSwabs (<https://www.copanusa.com>) for quantitative reverse transcription PCR (qRT-PCR) targeted to the viral envelope (E) and nucleocapsid (N) genes of SARS-CoV-2. Furthermore, we used virus isolation from lung tissue swabs from an additional cohort of deceased COVID-19 patients (n = 11) to compare molecular detection and virus cultivability (Appendix, <https://wwwnc.cdc.gov/EID/article/27/6/21-0226-App1.pdf>).

All patients were Caucasian, median age was 78 years (range 62–93 years), and 51.2% were female. The median disease duration (interval between the first positive SARS-CoV-2 PCR and death) was 11 days (range 1–43 days). The median postmortem interval (time between death and specimen sampling) was 23 hours (range 8–124 hours; Table; Appendix).

PCR is the current standard for SARS-CoV-2 detection (1,2). In our cohort, qRT-PCR targeted to the E gene showed a higher sensitivity than qRT-PCR for

Highly Pathogenic Avian Influenza A (H5N8) Virus in Swans, China, 2020

Appendix

Materials and Methods

Samples

Two sick swans, whooper swan (*Cygnus cygnus*) and mute swan (*Cygnus olor*) were found almost at the same site in Wuliangshuai Lake in Bayannur city, Inner Mongolia, China (41.826234°N, 107.54972°E) on 17 October 2020. The swans died soon and virus was detected and collected from organs at the same day. We collected multiple organs (brains, larynx, liver, lung, pancreas, kidney, spleen and rectum) from two dead swans. We sequenced the H5N8 genomes directly from organs, and we used them in whole genetic analysis. The egg passages were used to confirm the genome and to get the long-term preserved viral strains. We inoculated 10-day-old specific pathogen-free chicken embryos (National Poultry Laboratory Animal Resource Center, Harbin Veterinary Research Institute, Chinese Academy of Agriculture Sciences, Harbin 150069, China) with the homogenates of mixed organs, respectively. All chicken embryos dead within 48 hours, the allantoic fluid was harvested, and the hemagglutinin (HA) activity was assayed. Subtypes of influenza viruses were identified initially by using the hemagglutination inhibition (HI) test. Viral RNA was extracted from organs or HA positive samples from incubated allantoic fluid using a QIAamp Viral RNA Mini Kit (Qiagen, Germany), reverse transcribed using the primer Un12 and subjected to RT-PCR using the method described in the WHO manual (World Health Organization [WHO], 2002) to further confirm AIV positive. The PCR products of eight fragments of the isolates were sequenced using a set of specific sequencing primers listed in a previous dissertation (1). The sequence data were compiled using the SeqMan program (DNASTAR, Madison, WI, United States). Two H5N8 influenza viruses, A/whooper swan/Inner Mongolia/W1–1/2020(H5N8) and A/mute swan/Inner Mongolia/W2–1/2020(H5N8), were isolated.

Genetic Analysis

A BLASTn search was performed against sequences in the GISAID database to identify the closest relatives of the two Inner Mongolia H5N8 isolates (QH-H5N8) in early January 2021, and eight datasets were derived from the top 100 BLASTn hits. The genome of clade 2.3.4.4 H5N8 viruses isolated in 2020 were also downloaded. Sequences were aligned using MAFFT (2) implemented in PhyloSuite 1.21 (3). The alignment lengths for each dataset were: PB2 2,277 nt (nt), PB1 2,271 nt, PA 2,148 nt, HA 1,681 nt, NP 1,494 nt, NA 1,407 nt, M 979 nt, NS 835 nt. For all eight datasets, sequences without full alignment length were removed. We reconstructed the phylogenetic trees using selected representative sequences of 2.3.4.4 and sequences derived from GISAID. Maximum likelihood phylogenies were inferred using IQ-TREE (4) under the best-fit substitution model for 10000 ultrafast bootstraps (5). Best-fit substitution model was selected using the Bayesian information criterion by ModelFinder (6) implemented in PhyloSuite 1.21 (3).

References

1. Chai H. Molecular epidemiological study on influenza virus in wild birds of Heilongjiang. Harbin, China: Northeast Forestry University; 2012.
2. Katoh K, Standley DM. MAFFT multiple sequence alignment software version 7: improvements in performance and usability. *Mol Biol Evol.* 2013;30:772–80. [PubMed https://doi.org/10.1093/molbev/mst010](https://doi.org/10.1093/molbev/mst010)
3. Zhang D, Gao F, Jakovlić I, Zou H, Zhang J, Li WX, et al. PhyloSuite: An integrated and scalable desktop platform for streamlined molecular sequence data management and evolutionary phylogenetics studies. *Mol Ecol Resour.* 2020;20:348–55. [PubMed https://doi.org/10.1111/1755-0998.13096](https://doi.org/10.1111/1755-0998.13096)
4. Nguyen LT, Schmidt HA, von Haeseler A, Minh BQ. IQ-TREE: a fast and effective stochastic algorithm for estimating maximum-likelihood phylogenies. *Mol Biol Evol.* 2015;32:268–74. [PubMed https://doi.org/10.1093/molbev/msu300](https://doi.org/10.1093/molbev/msu300)
5. Minh BQ, Nguyen MA, von Haeseler A. Ultrafast approximation for phylogenetic bootstrap. *Mol Biol Evol.* 2013;30:1188–95. [PubMed https://doi.org/10.1093/molbev/mst024](https://doi.org/10.1093/molbev/mst024)

6. Kalyanamoorthy S, Minh BQ, Wong TKF, von Haeseler A, Jermini LS. ModelFinder: fast model selection for accurate phylogenetic estimates. *Nat Methods*. 2017;14:587–9. [PubMed](https://doi.org/10.1038/nmeth.4285)
<https://doi.org/10.1038/nmeth.4285>

Appendix Table 1. Virus isolates sharing the highest nucleotide similarity (top 2) with the two Inner Mongolia H5N8 isolates as identified on global initiative on sharing all influenza data (GISAID) in early January 2021

Segment	Virus name	Accession number*	similarity
A/whooper swan/Inner Mongolia/W1–1/2020(H5N8) [(A/mute swan/Inner Mongolia/W2–1/2020(H5N8))]			
PB2	A/Greylag goose/England/033100/2020(H5N8)	EPI1837929	99%
	A/barnacle goose/Sweden/SVA201117SZ0468/KN003355/2020(H5N8)	EPI1814739	99%
PB1	A/goose/Russia Novosibirsk region/1–12/2020(H5N8)	EPI1839239	99%
	A/domestic duck/Kazakhstan/1–274–20-B/2020(H5N8)	EPI1811615	99%
PA	A/domestic duck/Kazakhstan/1–274–20-B/2020(H5N8)	EPI1811615	99%
	A/goose/Russia Novosibirsk region/1–12/2020(H5N8)	EPI1839239	99%
HA	A/goose/Russia Novosibirsk region/1–12/2020(H5N8)	EPI1839239	99%
	A/domestic duck/Kazakhstan/1–274–20-B/2020(H5N8)	EPI1811615	99%
NP	A/duck/Russian Federation Omsk/1328–2/2020(H5N8)	EPI1811690	99%
	A/domestic duck/Kazakhstan/1–274–20-B/2020(H5N8)	EPI1811615	99%
NA	A/turkey/England/038115/2020(H5N8)	EPI1837953	99%
	A/turkey/England/037784/2020(H5N8)	EPI1837937	99%
M	A/barnacle goose/Sweden/SVA201117SZ0468/KN003355/2020(H5N8)	EPI1814739	99%
	A/Greylag_goose/England/033100/2020(H5N8)	EPI1837929	99%
NS	A/chicken/England/037052/2020(H5N8)	EPI1837911	99%
	A/Eurasian wigeon/Italy/20VIR7301–34/2020(H5N8)	EPI1815377	99%

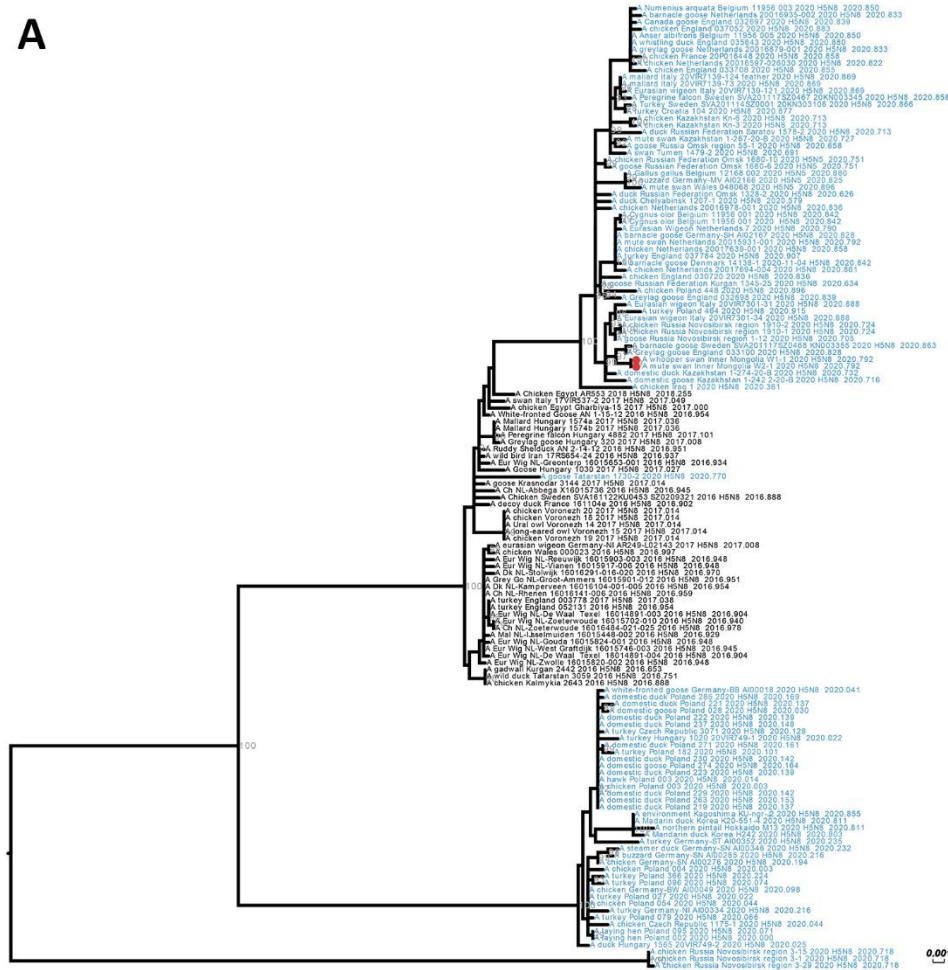
*EpiFlu Database of Global Initiative on Sharing All Influenza Data (GISAID).

Appendix Table 2. Information of viruses related the two Inner Mongolia isolates according to the HA genes

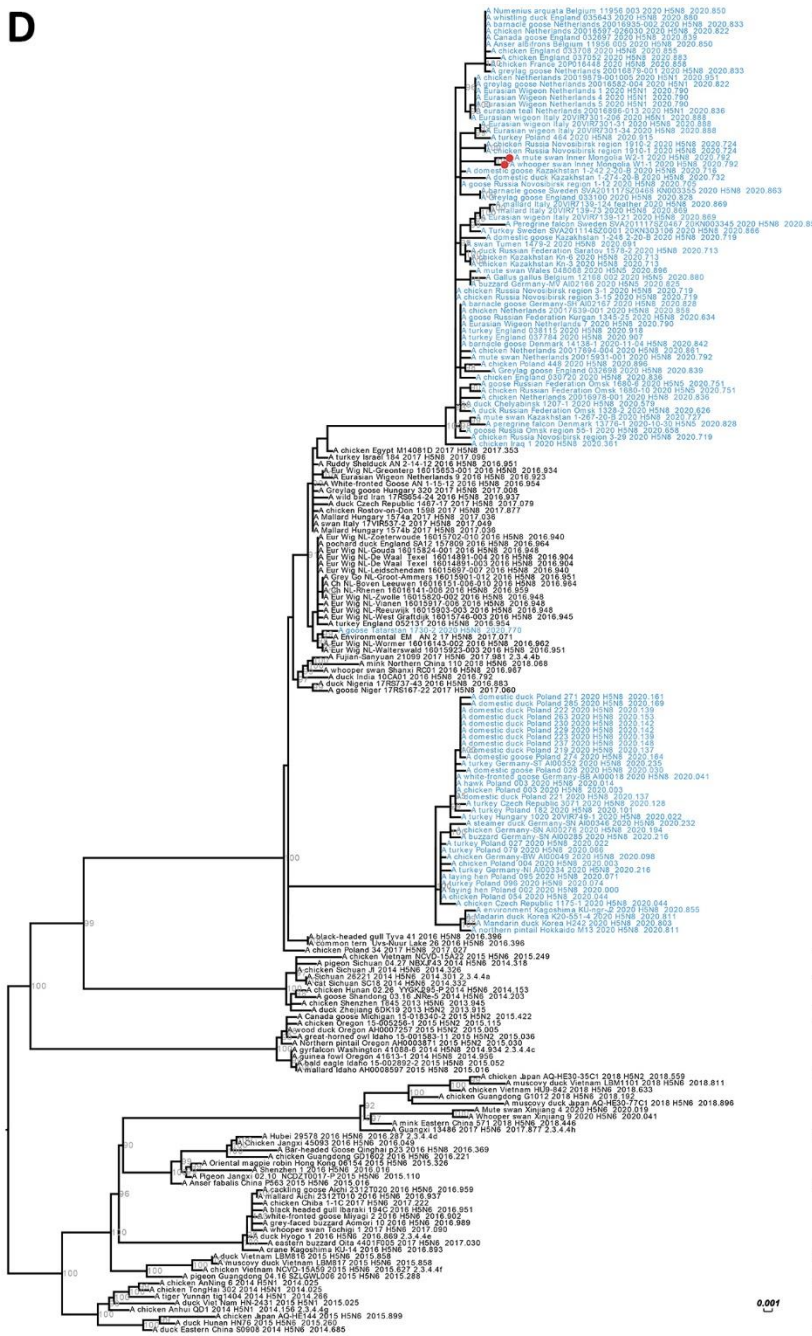
Date	Location	Isolate name	Isolate ID
2020-May-12	Iraq	A/chicken/Iraq/1/2020(H5N8)	EPI_ISL_623074
2020-Sep-18	Kazakhstan	A/chicken/Kazakhstan/Kn-3/2020(H5N8)	EPI_ISL_739686
2020-Sep-18	Kazakhstan	A/chicken/Kazakhstan/Kn-6/2020(H5N8)	EPI_ISL_739687
2020-Sep-19	Kazakhstan	A/domestic goose/Kazakhstan/1-242_2-20-B/2020(H5N8)	EPI_ISL_615073
2020-Sep-20	Kazakhstan	A/domestic goose/Kazakhstan/1-248_2-20-B/2020(H5N8)	EPI_ISL_615068
2020-Sep-22	Kazakhstan	A/domestic chicken/Kazakhstan/1-261_1-20-B/2020(H5N8)	EPI_ISL_615070
2020-Sep-23	Kazakhstan	A/mute swan/Kazakhstan/1-267-20-B/2020(H5N8)	EPI_ISL_614401
2020-Sep-25	Kazakhstan	A/domestic duck/Kazakhstan/1-274-20-B/2020(H5N8)	EPI_ISL_615072
2020-Jul-31	Russia	A/duck/Chelyabinsk/1207-1/2020(H5N8)	EPI_ISL_637098
2020-Aug-17	Russia	A/duck/Russian Federation Omsk/1328-2/2020(H5N8)	EPI_ISL_626650
2020-Sep-10	Russia	A/swan/Tumen/1479-2/2020(H5N8)	EPI_ISL_661178
2020-Sep-15	Russia	A/goose/Russia Novosibirsk region/1-12/2020(H5N8)	EPI_ISL_739684
2020-Sep-18	Russia	A/duck/Russian Federation/Saratov/1578-2/2020 (H5N8)	EPI_ISL_626649
2020-Sep-20	Russia	A/chicken/Russia Novosibirsk region/3-1/2020(H5N8)	EPI_ISL_739690
2020-Sep-20	Russia	A/chicken/Russia Novosibirsk region/3-15/2020(H5N8)	EPI_ISL_739691
2020-Sep-20	Russia	A/chicken/Russia Novosibirsk region/3-29/2020(H5N8)	EPI_ISL_739692
2020-Sep-22	Russia	A/chicken/Russia Novosibirsk region/1910-1/2020(H5N8)	EPI_ISL_739688
2020-Sep-22	Russia	A/chicken/Russia Novosibirsk region/1910-2/2020(H5N8)	EPI_ISL_739689
2020-Oct-02	Russia	A/chicken/Russian Federation/Omsk/1680-10/2020(H5N5)	EPI_ISL_626647
2020-Oct-02	Russia	A/goose/Russian Federation/Omsk/1680-6/2020(H5N5)	EPI_ISL_626648
2020-Oct-16	Netherlands	A/Eurasian Wigeon/Netherlands/1/2020(H5N1)	EPI_ISL_603133
2020-Oct-16	Netherlands	A/Eurasian Wigeon/Netherlands/4/2020(H5N1)	EPI_ISL_603134
2020-Oct-16	Netherlands	A/Eurasian Wigeon/Netherlands/5/2020(H5N1)	EPI_ISL_603135
2020-Oct-16	Netherlands	A/Eurasian Wigeon/Netherlands/7/2020(H5N8)	EPI_ISL_603136
2020-Oct-17	Netherlands	A/mute swan/Netherlands/20015931-001/2020(H5N8)	EPI_ISL_591075
2020-Oct-28	Netherlands	A/chicken/Netherlands/20016597-026030/2020(H5N8)	EPI_ISL_603132
2020-Oct-28	Netherlands	A/greylag goose/Netherlands/20016582-004/2020(H5N1)	EPI_ISL_632314
2020-Nov-01	Netherlands	A/barnacle goose/Netherlands/20016935-002/2020(H5N8)	EPI_ISL_632317
2020-Nov-01	Netherlands	A/greylag goose/Netherlands/20016879-001/2020(H5N8)	EPI_ISL_632318
2020-Nov-02	Netherlands	A/Eurasian teal/Netherlands/20016896-013/2020(H5N1)	EPI_ISL_632315
2020-Nov-02	Netherlands	A/chicken/Netherlands/20016978-001/2020(H5N8)	EPI_ISL_641377
2020-Nov-10	Netherlands	A/chicken/Netherlands/20017639-001/2020(H5N8)	EPI_ISL_641394
2020-Nov-11	Netherlands	A/chicken/Netherlands/20017694-004/2020(H5N8)	EPI_ISL_641395
2020-Dec-14	Netherlands	A/chicken/Netherlands/20019879-001005/2020(H5N1)	EPI_ISL_711055
2020-Oct-29	Germany	A/buzzard/Germany-MV/AI02166/2020(H5N5)	EPI_ISL_614399
2020-Oct-30	Germany	A/barnacle goose/Germany-SH/AI02167/2020(H5N8)	EPI_ISL_614400
2020-Oct-30	Denmark	A/peregrine falcon/Denmark/13776-1/2020-10-30(H5N5)	EPI_ISL_644737
2020-Nov-04	Denmark	A/barnacle goose/Denmark/14138-1/2020-11-04(H5N8)	EPI_ISL_644824
2020-Oct-30	England	A/Greylag goose/England/033100/2020(H5N8)	EPI_ISL_710508
2020-Nov-02	England	A/chicken/England/030720/2020(H5N8)	EPI_ISL_626652
2020-Nov-03	England	A/Canada goose/England/032697/2020(H5N8)	EPI_ISL_710506
2020-Nov-03	England	A/Greylag goose/England/032698/2020(H5N8)	EPI_ISL_710507
2020-Nov-09	England	A/chicken/England/033708/2020(H5N8)	EPI_ISL_710509
2020-Nov-18	England	A/whistling duck/England/035643/2020(H5N8)	EPI_ISL_710512
2020-Nov-19	England	A/chicken/England/037052/2020(H5N8)	EPI_ISL_710511
2020-Nov-24	England	A/mute swan/Wales/048068/2020(H5N5)	EPI_ISL_683999
2020-Nov-28	England	A/turkey/England/037784/2020(H5N8)	EPI_ISL_710504
2020-Dec-02	England	A/turkey/England/038115/2020(H5N8)	EPI_ISL_710505
2020-Nov-04	Belgium	A/Cygnus olor/Belgium/11956_001/2020(H5N8)	EPI_ISL_644735
2020-Nov-07	Belgium	A/Numenius arquata/Belgium/11956_003/2020(H5N8)	EPI_ISL_664102
2020-Nov-07	Belgium	A/Anser albifrons/Belgium/11956_005/2020(H5N8)	EPI_ISL_661313
2020-Nov-18	Belgium	A/Gallus gallus/Belgium/12168_002/2020(H5N5)	EPI_ISL_660264
2020-Nov-10	Sweden	A/Peregrine falcon/Sweden/SVA201117SZ0467/20KN003345/2020(H5N8)	EPI_ISL_668456
2020-Nov-12	Sweden	A/barnacle goose/Sweden/SVA201117SZ0468/KN003355/2020(H5N8)	EPI_ISL_668457
2020-Nov-13	Sweden	A/Turkey/Sweden/SVA201114SZ0001/20KN303106/2020(H5N8)	EPI_ISL_647969
2020-Nov-10	France	A/chicken/France/20P016448/2020(H5N8)	EPI_ISL_667810
2020-Nov-14	Italy	A/mallard/Italy/20VIR7139-124_feather/2020(H5N8)	EPI_ISL_683594
2020-Nov-14	Italy	A/mallard/Italy/20VIR7139-73/2020(H5N8)	EPI_ISL_654958
2020-Nov-14	Italy	A/Eurasian wigeon/Italy/20VIR7139-121/2020(H5N8)	EPI_ISL_683593
2020-Nov-21	Italy	A/Eurasian wigeon/Italy/20VIR7301-206/2020(H5N1)	EPI_ISL_683592
2020-Nov-21	Italy	A/Eurasian wigeon/Italy/20VIR7301-31/2020(H5N8)	EPI_ISL_683751
2020-Nov-21	Italy	A/Eurasian wigeon/Italy/20VIR7301-34/2020(H5N8)	EPI_ISL_683752
2020-Nov-24	Poland	A/chicken/Poland/448/2020(H5N8)	EPI_ISL_661177
2020-Dec-01	Poland	A/turkey/Poland/464/2020(H5N8)	EPI_ISL_779129

Appendix Figure. Maximum-likelihood phylogenetic trees. Our Inner Mongolia H5N8 isolates were marked with red circle and viruses isolated in 2020 are shown in blue. A UFBoot support values ≥ 90 was shown. Segments shown: A) polymerase basic; B) polymerase basic; C) polymerase; D) hemagglutinin; E) nucleoprotein; F) neuraminidase; G) matrix protein; H) nonstructural protein.

A



D



2.3.4.4b

2.3.4.4a

2.3.4.4c

2.3.4.4h

2.3.4.4d

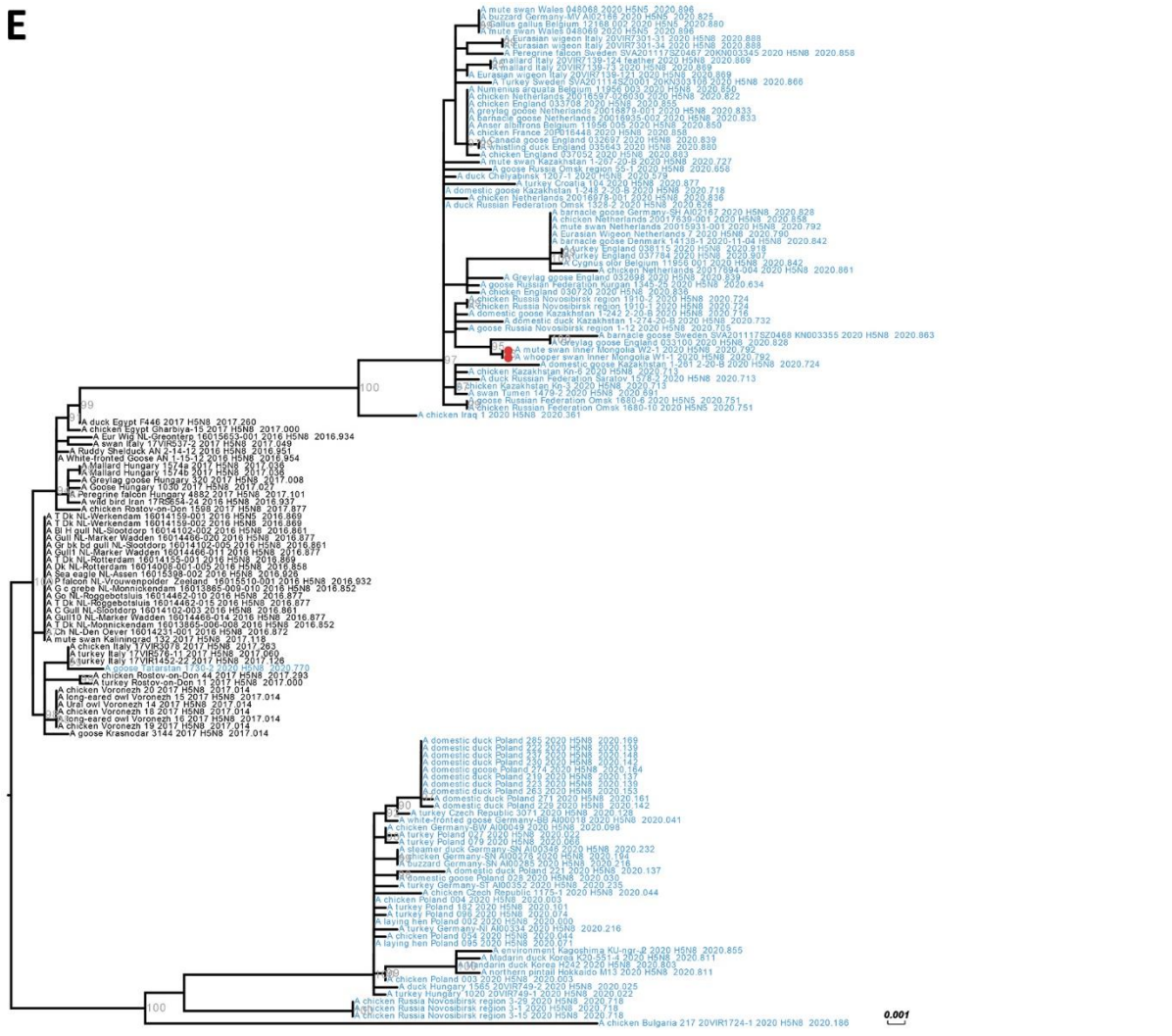
2.3.4.4e

2.3.4.4f

2.3.4.4g

0.001

E



F

